Laminar kinetic energy model based on the Klebanoff-mode dynamic to predict bypass transition on a turbine blade

Loïc Jecker, Olivier Vermeersch, Hugues Deniau, E. Croner, Grégoire Casalis

LAMINAR KINETIC ENERGY MODEL BASED ON THE KLEBANOFF-MODE DYNAMIC TO PREDICT BYPASS TRANSITION ON A TURBINE BLADE

L. Jecker[1,2], *O. Vermeersch*[1], *H. Deniau*[1], *E. Croner*[2] *and G. Casalis*[3]

[1] *ONERA DMPE, 2 av. Edouard Belin, 31055 Toulouse, France*
[2] *Safran Tech, 78772 Magny-les-Hameaux, France*
[3] *ISAE-SUPAERO, 31055 Toulouse, France*

loic.jecker@onera.fr

Abstract

This paper deals with the application of a bypass-transition model developed by Jecker *et al.* (2017) (JVD), using the laminar kinetic energy (LKE) concept. JVD formulation is written to model the Klebanoff-mode dynamic with an original definition of the LKE and a physics-based associated equation.
The application case is the von Kármán Institute's (VKI) LS89 turbine blade, Arts *et al.* (1990).

1 Bypass transition scenario

The bypass transition is characterised by the formation of low-frequency, high-velocity streak-shaped disturbances - up to 30% of the mean-flow velocity, Andersson *et al.* (1999) - called Klebanoff modes (K. modes). Theses instabilities are considered by several authors as the key phenomenon of the bypass transition, see for instance Durbin (2017).

The bypass-transition scenario is decomposed into five steps, Jacobs *et al.* (2001). The 1st step is the receptivity step and describes how the free-stream turbulence (FST) enters the boundary layer. These vortices then interact with the boundary-layer shear to form the streaks (step 2). This is called the *lift-up* mechanism, identified by Landahl (1980). It consists in a mean-flow momentum displacement caused by the wall-normal part of the FST: the higher velocities from the upper part of the boundary layer move towards the wall while the lower velocities rise to the boundary layer edge. When the streak reaches a significant amplitude, it is destabilised (step 3). The 4th step consists in the formation of turbulent spots by the unstable streaks' breakdown. These spots may grow or disappear and finally occupy the whole boundary layer (step 5).

2 Development of a new model

Klebanoff mode modelling

A bypass-transition model was developed by the authors, Jecker *et al.* (2017), based on the LKE concept proposed by Mayle & Schulz (1997) and popularised by Walters & Cokljat (2008) (WC) with their $k_T - k_L - \omega$ formulation. WC formulation uses the Boussinesq hypothesis for both turbulent and laminar velocity fluctuations. They defined two different eddy viscosities based on a separation between the "large" coherent eddies from the small turbulent scales.
The authors chose to change the definition of the LKE. They defined the LKE as the streamwise kinetic energy of the K. modes. They wrote a transport equation for the LKE k_L from the linearised Navier-Stokes equations, satisfied by the streamwise velocity fluctuation u_{st} of the K. modes. The k_L production term P_{k_L} is written to model the lift-up phenomenon in the laminar boundary layer, so that it is proportional to $P_{k_L} \propto -\overline{u_{st}v'}$. The wall-normal velocity fluctuation energy v'^2 is considered proportional to the turbulent kinetic energy k_T. This leads to :

$$k_L = \frac{\overline{u_{st}^2}}{2},\ P_{k_L} = \alpha\sqrt{k_L k_T}S. \tag{1}$$

S is the strain rate tensor magnitude and $\alpha = 0.063$ is a constant of the model. The transition onset is detected by a criterion, comparing the LKE value to the mean-flow shear, in accordance with Jacobs & Durbin (2001) analysis of streak destabilisation on direct simulations:

$$\frac{k_L + 3k_T}{\nu S} > C_{onset}. \tag{2}$$

$C_{onset} = 11$ is a constant of the model. The addition of $3k_T$ to k_L is done so that the criterion is still verified in the turbulent boundary layer. In the transition region, k_L is more than ten times higher than k_T, this addition thus does not influence the transition onset position.

Transition onset calculation

Once the transition criterion is verified, the energy transfer from the laminar fluctuations - K. modes (k_L) - to the turbulent spots (k_T) is controlled by a transfer term T_k, defined as:

$$T_k = f_{tr} C_T k_L S. \tag{3}$$

$C_T = 0.015$ is a constant of the model. This term will appear both in k_L and k_T equations with opposite sign.

It involves a transition function f_{tr}, calculated with an additional transport equation:

$$\frac{D\rho\beta}{Dt} = \rho C_\beta f_{crit}\left(1-\beta\right)S, \tag{4}$$

where $f_{crit} = 1$ if the criterion is verified - $f_{crit} = 0$ otherwise - and $C_\beta = 0.013$ is a constant of the model. The transition function is thus defined as the maximum of β along the wall-normal direction:

$$f_{tr} = \max_d\left(\beta\right), \tag{5}$$

with d the distance to the wall. Additionally, a turbulent indicator is used to separate the laminar zone to the transitional and turbulent regions. It is defined as:

$$\beta_{BP} = 1 - e^{-100 f_{tr}}. \tag{6}$$

In the laminar boundary layer, $\beta_{BP} = 0$; once the criterion is verified, β_{BP} rises abruptly to 1.

Influence of K. modes on the mean flow

As mentioned previously, K. modes can reach large amplitude so that they can deeply influence the mean flow. This impact on the mean flow is accounted for by an anisotropic Reynolds tensor:

$$\overline{u_i u_j} = \overline{u_i' u_j'} + \overline{u_i u_j}_{st}, \tag{7}$$

$$\overline{u_i u_j}_{st} = \begin{pmatrix} 2k_L & -\alpha\sqrt{k_L k_T} & 0 \\ -\alpha\sqrt{k_L k_T} & 0 & 0 \\ 0 & 0 & 0 \end{pmatrix}. \tag{8}$$

The turbulent tensor $\overline{u_i' u_j'}$ is given by the turbulence modelling.

In the LS89 test case, only the heat transfer was measured. So far JVD model did not contain a heat transfer modelling. As a first approach, it is proposed to model the heat flux vector $\overline{u_i\theta}$ with a Simple Gradient Diffusion Hypothesis (SGDH). It is based on a modified turbulent diffusivity α_θ taking account of a streak effect:

$$-\overline{u_i\theta} = \alpha_\theta\frac{\partial T}{\partial x_i},\ \alpha_\theta = \frac{\nu_t}{Pr_t} + C_\theta\frac{2k_L}{SPr_t}, \tag{9}$$

with the turbulent Prandtl number $Pr_t = 0.85$.

Full formulation

The turbulence modelling rests on the Boussinesq hypothesis:

$$\overline{u_i' u_j'} = \frac{2}{3}k_T\delta_{ij} - 2\nu_T S_{ij}, \tag{10}$$

with the following eddy viscosity:

$$\nu_T = f_\nu C_\mu f_W^2\frac{k_T}{\omega}. \tag{11}$$

The f_ν, C_μ and f_W functions come from the Walters & Cokljat (2008) model:

$$f_\nu = 1 - \exp\left(-\frac{f_W\sqrt{R_T}}{A_\nu}\right),\ R_T = \frac{k_T}{\nu\omega}, \tag{12}$$

$$C_\mu = \frac{1}{A_0 + A_S S\omega^{-1}},\ \lambda_T = \frac{\sqrt{k_T}}{\omega}, \tag{13}$$

$$\lambda_{eff} = \min\left(C_\lambda d, \lambda_T\right),\ f_W = \left(\frac{\lambda_{eff}}{\lambda_T}\right)^{2/3}. \tag{14}$$

The equation for k_L, k_T and ω are the following:

$$\begin{cases} \dfrac{D\left(\rho k_L\right)}{Dt} = \rho P_{k_L} - \rho T_k - 2\mu\left(\dfrac{\partial\sqrt{k_L}}{\partial x_j}\right)^2 + \dfrac{\partial}{\partial x_j}\left[\mu\dfrac{\partial k_L}{\partial x_j}\right], \\ \dfrac{D\left(\rho k_T\right)}{Dt} = \rho P_{k_T} + \rho T_k - \rho\omega k_T - 2\mu\left(\dfrac{\partial\sqrt{k_T}}{\partial x_j}\right)^2 + \dfrac{\partial}{\partial x_j}\left[\left(\mu + \dfrac{\rho\alpha_T}{\sigma_k}\right)\dfrac{\partial k_T}{\partial x_j}\right], \\ \dfrac{D\left(\rho\omega\right)}{Dt} = C_{\omega,1}\dfrac{\rho\omega}{k_T}P_{k_T} + \rho\left(\dfrac{C_{\omega,R}}{f_W} - 1\right)\dfrac{\omega}{k_T}T_k - \rho C_{\omega,2}f_W^2\omega^2 + \dfrac{\partial}{\partial x_j}\left[\left(\mu + \dfrac{\rho\alpha_T}{\sigma_\omega}\right)\dfrac{\partial\omega}{\partial x_j}\right]. \end{cases} \tag{15}$$

The k_L production term is defined as:

$$P_{k_L} = \left[\left(1-\beta_{BP}\right) + \beta_{BP}f_L\right]\alpha\sqrt{k_L k_T}S, \tag{16}$$

with f_L a damping function so that P_{k_L} disappears in the turbulent region:

$$f_L = \max\left(0, 1 - 1.1 f_{tr}\right). \tag{17}$$

The turbulent kinetic energy (TKE) k_T production term is written:

$$\begin{aligned} P_{k_T} &= \left(1-\beta_{BP}\right)k_T\omega \\ &\quad +\beta_{BP}f_{tr}f_\nu C_\mu f_p^2\frac{k_T}{\omega}S^2. \end{aligned} \tag{18}$$

Therefore, k_T does not grow in the laminar boundary layer, where $\beta_{BP} = 0$. The use of f_p is justified by

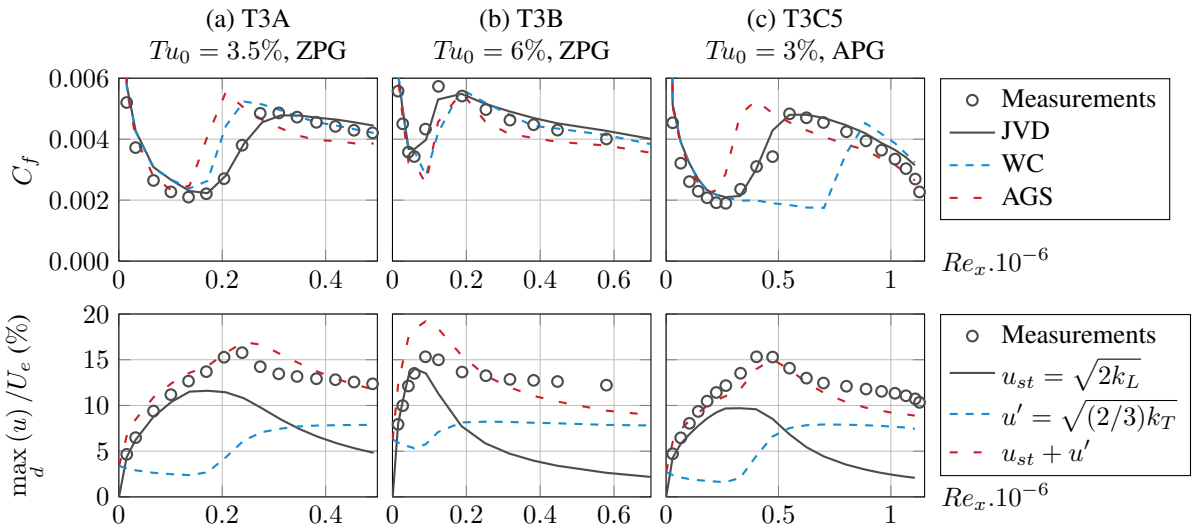

Figure 1: Superior part: evolution of the skin friction coefficient for ERCOFTAC T3 cases, T3A (a) and T3B (b) with a zero pressure gradient (ZPG) and T3C5 (c) exposed to an adverse pressure gradient (APG). Inferior part: evolution of the wall-normal maximum of the velocity fluctuations in the same cases.

$C_{\mu,std} = 0.09$	$C_{\omega,1} = 0.44$
$C_\lambda = 2.495$	$C_{\omega,2} = 0.92$
$A_\nu = 6.75$	$C_{\omega,R} = 1.5$
$\sigma_k = 1.0$	$\sigma_\omega = 1.17$
$A_0 = 4.04$	$A_S = 2.12$

$\alpha = 0.063$	$C_{onset} = 11$
$C_T = 1.5 \times 10^{-2}$	$C_\beta = 1.3 \times 10^{-2}$

Table 1: The constants for the turbulent region - from Walters & Cokljat (2008) - are displayed on the superior table, and the constants for the laminar and transition regions on the inferior table.

the TKE growth in the transition region:

$$f_p = \max\left(f_W, 1 - 0.7\exp\left(-\sqrt{\frac{Re_y}{37}}\right)\right), \qquad Re_y = \frac{y\sqrt{k_T}}{\nu}. \tag{19}$$

The turbulent viscosity used in the turbulent diffusion is defined as:

$$\alpha_T = f_\nu C_{\mu,std} f_W^2 \frac{k_T}{\omega}. \tag{20}$$

The constants of the model are gathered in Table 1.

The model was validated and its constants were calibrated using the ERCOFTAC T3 - A, B and C1 to C5 - cases, Roach *et al.* (1992). To illustrate the results obtained, the skin friction coefficients measured in three T3 cases is presented in figure 1. The T3A (a) and T3B (b) cases have a zero pressure gradient and are subjected to different FST levels. The T3C5 case (c) has an adverse pressure gradient, it is the most representative of the flow around a turbine blade. The measurements are compared to the predictions of JVD model, WC model and to the Abu-Ghannam and Shaw (1980) criterion (AGS). The wall-normal maximum of the longitudinal velocity perturbation measured in the ERCOFTAC T3A, T3B and T3C5 cases is presented in the inferior part of the figure 1. It is compared to the calculated normalised amplitude of the streak u_{st}, of the turbulence u' and of the total velocity fluctuation $u_{st} + u'$.

3 Application to a turbine blade

JVD model was applied to the VKI LS89 turbine blade, Arts *et al.* (1990). This case is frequently used to investigate turbomachinery transition models. Three configurations were tested: MUR217, MUR235 and MUR237. In these three cases, the elevation of the heat transfer in the pre-transitional zone seems to indicate that strong disturbances may exist in this region. These disturbances could be streaks.

Table 2 presents the inlet total pressure Pi_1, the outlet static pressure P_2 and the inlet turbulence level Tu_0 in the tested cases. The inlet Mach number in the three cases is $M = 0.15$. The MUR217 and MUR235 have approximately the same inlet total pressure and the same outlet static pressure, but a different turbulence level.

Case	Pi_1 (Pa)	P_2 (Pa)	Tu_0
MUR217	183500	104500	3.9%
MUR235	182800	104900	5.3%
MUR237	175300	117900	5.3%

Table 2: Numerical parameters for the VKI LS89, Arts *et al.* (1990)

Turbulence inlet conditions

Experimentally, the FST is generated by a grid, Arts (1990). In order to have different values of inflow turbulence Tu_0 at 55 mm upstream the leading edge, the grid was moved at different locations. This allowed to obtain four distinct turbulence levels, 5.3%, 3.9%, 3.1% and 2.5%, Fontaneto (2014). The turbulence levels are plotted in figure 2 as functions of the relative grid distance x.

The turbulence inlet parameters, k_0 and ω_0, are calculated in order to fit the measured turbulence evolution. The knowledge of the turbulence level as a function of the relative grid distance x enables the determination of the turbulence dissipation rate. Far upstream from the model, the equations for k_T and ω become:

$$\begin{aligned} U_0 \frac{\partial k_T}{\partial x} &= -k_T \omega, \\ U_0 \frac{\partial \omega}{\partial x} &= -C_{\omega,2} \omega^2. \end{aligned} \tag{21}$$

This system has the following solutions:

$$\begin{aligned} \frac{\omega}{\omega_0} &= \left(1 + C_{\omega,2} \frac{\omega_0 x}{U_0}\right)^{-1}, \\ \frac{k_T}{k_{T,0}} &= \left(\frac{\omega}{\omega_0}\right)^{1/C_{\omega,2}}. \end{aligned} \tag{22}$$

The inlet condition can be written on Tu and μ_t/μ with the following definitions:

$$Tu = \frac{1}{U}\sqrt{\frac{2}{3}k_T}, \quad \mu_t = \rho \frac{C_{\mu,std} k_T}{\omega}. \tag{23}$$

The three configurations have approximately the same inlet velocity of $U_0 = 61$ m/s. The choice of $\mu_t/\mu = 140$ for an inlet turbulence level of $Tu_0 = 5.3\%$ fits the measurements, as displayed in figure 2. The inlet condition for the MUR217 and MUR235 configurations is consequently $Tu_0 = 5.3\%$ and $\mu_t/\mu = 140$ at a distance of 55 mm upstream the leading edge. The inlet condition for the MUR217 configuration is $Tu_0 = 3.9\%$ and $\mu_t/\mu = 132$ at the same location.

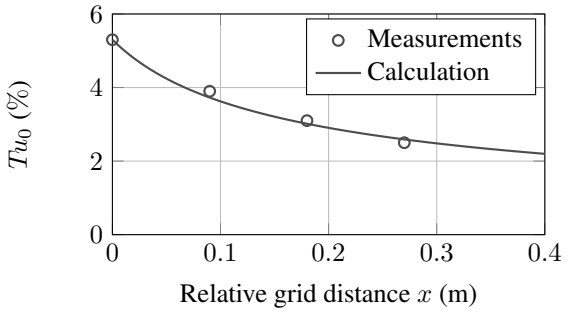

Figure 2: Inflow turbulence level Tu_0 in the LS89 case as a function of the relative grid distance x, Fontaneto (2014). The calculation is done with $Tu_0 = 5.3\%$, $U_0 = 61$ m/s and $\mu_t/\mu = 140$.

Streak diffusivity calibration

The coefficient C_θ used in equation (9) to model the influence of the streaks on the thermal fluxes is not yet determined. Since no academic cases are available in the literature, this constant was determined using one of the LS89 cases. $C_\theta = 300$ was chosen so that $C_\theta\,(2k_L/S)$ is - in the pre-transitional zone - of an order of magnitude comparable to ν_t - in the turbulent boundary layer.

Numerical results

Figure 3 represents the heat transfer measured for the three configurations, and calculated with JVD model in elsA software, Cambier & Gazaix (2002). First, the simulations underpredict the heat transfer of about 150 W/m2/K in the laminar region. This shift will not be discussed here since it is not caused by the transition model. These results are used qualitatively to analyse the behaviour of JVD model.

Numerically the transition onset is predicted at the same position in the MUR217 and MUR235 cases and corresponds to the shock location - around $s \sim 0.07$ m, with s the curvilinear abscissa - as represented by the evaluation of the isentropic Mach number M_{is} in figure 4:

$$M_{is} = \sqrt{\frac{2}{\gamma - 1}\left[\left(\frac{p_i}{p}\right)^{\frac{\gamma-1}{\gamma}} - 1\right]}. \tag{24}$$

The total pressure is written p_i, p represents the static pressure and $\gamma = 1.4$ the ratio of specific heats. Experimentally, the heat-transfer measurements on the MUR235 configuration have the following features, not reproduced by the simulation: an earlier transition, a pre-transitional region where the heat transfer begins to rise and a wider extent of the transitional region. In the MUR237 case a pre-transitional region is also observable. It is predicted by the model, although the heat-transfer is sightly underestimated. Contrary to the MUR217 and MUR235 configurations, the transition on MUR237 is not triggered by the shock. The transition is predicted by the model, however too late and the transition extent is too short.

On the pressure side, the MUR217, MUR235 and MUR237 configurations show a similar behaviour. The heat transfer first decreases as the flow accelerates, then increases for $|s| > 0.025$ m until it reaches a maximum for $|s| \sim 0.055$ m and decreases again in the trailing edge region. The heat transfer predicted by the simulation decreases also with the flow acceleration. However, it begins to rise earlier and reaches its maximum earlier. This local maximum happens later in the MUR217 case than in the MUR235 and MUR237 cases. After a second decrease it rises once again.

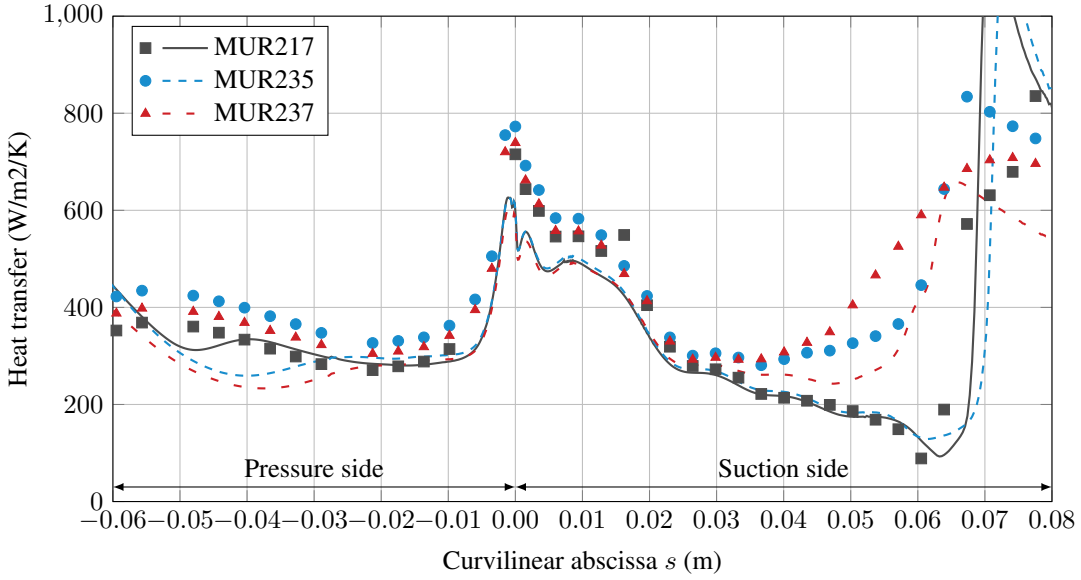

Figure 3: Heat transfer for three configurations of the VKI LS89 turbine blade, Arts *et al.* (1990). The symbols depict the measurements and the lines the calculations.

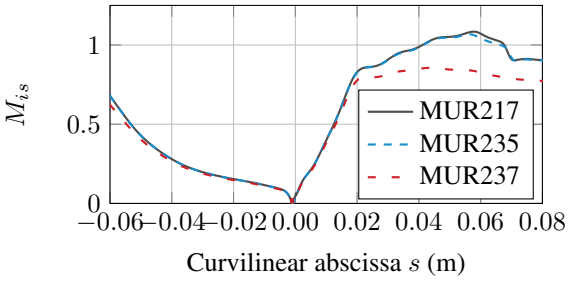

Figure 4: Isentropic Mach number M_{is} for three configurations of the VKI LS89 turbine blade, Arts *et al.* (1990).

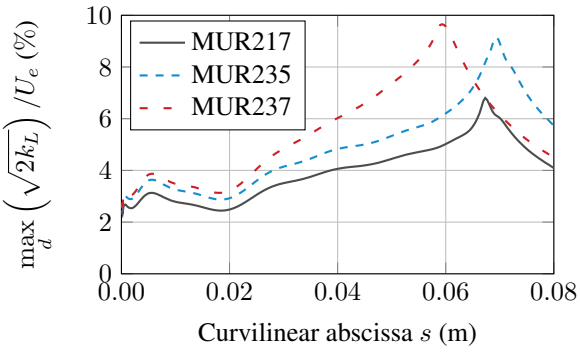

Figure 5: Streak amplitude in the tested LS89 cases.

4 Discussion

The results of the application of JVD model on the LS89 turbine blade show two discrepancies. First, the model does not accurately predict the heat transfer elevation in the pre-transitional region on the MUR235 and MUR237 configurations. Secondly, the model predicts too late a transition onset and too short a transition region extent on the same configurations.

Pre-transitional region

The cause of the elevation of the heat transfer in the pre-transitional region is not well understood. According to Cação Ferreira *et al.* (2017), these disturbances are associated to turbulent spots. However, another possibility is that streaks are responsible for this heat transfer elevation. There are consequently two questions that need to be resolved. Firstly, could streaks be responsible for this augmentation? Secondly, is the influence of the streaks on the heat transfer well taken into account by the model?

In order to answer the first question, the streak amplitude $\max_d \left(\sqrt{2k_L}\right)$ divided by the external velocity U_e is displayed in figure 5 for the three tested configurations. The model predicts in the MUR237 case a streak amplitude of a similar order of magnitude than the one calculated in the ERCOFTAC T3C5 case, figure 1. Streaks are thus predicted by the model in the laminar boundary layer. Moreover, a raise of the streak amplitude occurs at the same position than an elevation of the heat transfer is noticed on the experiments, $s \sim 0.027$ m. The existence of streaks is thus predicted by the model, with an amplitude comparable to the one observed in academic cases.

Streaks can influence the heat transfer through two mechanisms, that will be considered in order to answer the second question. The first one is an indirect mechanism, it consists in the modification of the mean velocity profile due to the streaks. The influence of the streaks on the mean velocity flow is noticeable on the shape factor or on the skin friction coefficient evolution in the laminar boundary layer in bypass transition cases. Since the mean velocity influences the heat transfer, and since the streaks influence the mean

velocity flow, the streaks indirectly influence the heat transfer. This mechanism is taken into account by the model through the modified Reynolds tensor, equation (8). The second effect comes from the fact that streaks are streamwise vortices, they may thus increase the mixing in the near wall region and consequently increase the heat transfer. This influence is modelled through the $\overline{u_i\theta}$ term, equation (9), which has not been calibrated using academic cases in JVD model.

Transition onset and extent

The predicted streak amplitude in the MUR237 case is comparable to the one predicted in the ERCOFTAC T3C5 case in figure 1. On the contrary, the predicted streak amplitude in the MUR217 case is too low for the criterion to detect a transition. Moreover, the u_{st}/U_e value calculated for MUR235 at the transition onset is close to the one observed for MUR237. It is not high enough so that the criterion detects a transition, it is however not far.
The streamwise evolution of the skin friction coefficients displayed in figure 1 shows a similar behaviour in the T3A (a) and T3C5 (c) cases, the transition onset is predicted slightly too late and the transition extent is too short. A possible modification of the model could be to lower the criterion threshold value and to slow down the transition dynamic.

5 Conclusion

JVD model is a RANS bypass-transition model based on the dynamic of Klebanoff modes which is represented by an additional transported variable - the laminar kinetic energy, k_L. It has been validated on academic configurations and showed a physically accurate dependence to the turbulence intensity of the external flow, to its turbulent length scale and to the external pressure gradient, Jecker *et al.* (2017).
The model was for the first time applied to a turbine blade test case, three configurations of the LS89 case were simulated. The numerical results showed differences with the heat transfer measurements. The transition onset is predicted too late, the transition extent is too short and the heat transfer elevation in the pre-transitional region is not accurately predicted. However, the streak amplification is predicted in the laminar zone. A lower criterion threshold value and a slower transition dynamic could improve the transition prediction. Concerning the heat transfer elevation in the pre-transitional region, the modelling of the streak's direct influence on the temperature is probably responsible for this difference. An improvement could consist in writing an additional transport equation for the $\overline{u_{st}\theta}$ term, as done by Vermeersch *et al.* (2010).

Acknowledgments

This work has been founded by SAFRAN group.

References

Andersson P., Berggren M., Henningson D.S. (1999), Optimal disturbances and bypass transition in boundary layers, *Physics of Fluids*, Vol. 11, pp. 134–150

Arts T., Lambert de Rouvroit M. and Rutherford A.W. (1990), Aero-thermal investigation of a highly loaded transonic linear turbine guide vane cascade, VKI Technical Report

Cação Ferreira T. and Arts T. (2017), Influence of gas-to-wall temperature ratio on by-pass transition, ASME Turbo Expo 2017: Turbomachinery Technical Conference and Exposition

Cambier L. and Gazaix M. (2002), elsA – An efficient object-oriented solution to CFD complexity, 40th AIAA Aerospace Sciences Meeting & Exhibit

Durbin P.A. (2017), Perspectives on the Phenomenology and Modeling of Boundary Layer Transition, *Flow, Turbulence and Combustion*, pp. 1–23

Fontaneto F. (2014), Aero-thermal Performance of a Film-cooled High Pressure Turbine Blade / Vane: a Test Case for Numerical Codes Validation, Ph.D. thesis, von Kármán Institute

Jacobs R.G. and Durbin P.A. (2001), Simulations of bypass transition, *Journal of Fluid Mechanics*, Vol. 428, pp. 185–212

Jecker L., Vermeersch O., Deniau H., Casalis G. and Croner E. (2017), A New Laminar Kinetic Energy Model for RANS Simulations of Bypass Transition, 47th AIAA Fluid Dynamics Conference

Landahl MT. (1980), A note on an algebraic instability of inviscid parallel shear flows, *Journal of Fluid Mechanics*, Vol. 98, pp. 243–251

Mayle R.E. and Schulz A. (1997), The Path to Predicting Bypass Transition, *Journal of Turbomachinery*, Vol. 119, pp. 405–411

Roach P.E. and Brierley D.H. (1992), The influence of a turbulent free-stream on zero pressure gradient transitional boundary layer development. Part I: Test cases T3A and T3B, *Numerical simulation of unsteady flows and transition to turbulence*, pp. 319–347

Vermeersch O. and Arnal D. (2010), Klebanoff-mode modeling and bypass-transition prediction, *AIAA Journal*, Vol. 48, pp. 2491–2500

Walters D.K. and Cokljat D. (2008), A Three-Equation Eddy-Viscosity Model for Reynolds-Averaged Navier–Stokes Simulations of Transitional Flow, *Journal of Fluids Engineering*, Vol. 130